Creep-Fatigue Life Prediction – A Ductility Model

Tarun Goswami

Research Assistant Professor
Mechanical Engineering Department
University of Utah, Salt Lake City, UT 84112 USA

ABSTRACT

Creep-fatigue life prediction methods are briefly reviewed. Phenomenological methods of life prediction are very popular, since they use several test and metallographic parameters in model formulation. They also require numerous test parameters determined from specialized tests. Requirements of phenomenological methods have been summarized. Ductility measurement and modeling aspects have been reviewed. A new model has been developed with the assumption that with increasing fatigue cycles the ductility gradually decreases and the specimen fails as a result of exhaustion of ductility. This has been achieved in terms of dynamic viscosity (product of stress and cycle time), equated with material toughness, which is a product of material strength and ductility. There is a limiting value of ductility and yield to tensile strength ratio, where this method applies.

Creep-fatigue data on five 'test materials', namely AMZIRC, Ti-6Al-4V, IN 100, Waspaloy and 1Cr-Mo-V steels, have been assessed with the proposed method. Nearly 70% of the test data points with or without hold times were predicted within a factor of ± x 2.

NOMENCLATURE

N = Number of cycles at specified conditions.

N_f = number of cycles to failure at the specified condition of N.

t = Time of hold at specified conditions.

t_r = Time to creep-rupture at the specified conditions of t.

N_{ij} = Cyclic life under ij conditions where ij may be PP, PC, CP and CC.

A_{ij} = Intercept of inelastic strain life curve.

ν = Frequency and subscript t and c for tension and compression.

k = Slope of frequency (strain rate) versus endurance line

β' = Slope of plastic strain range versus cyclic life.

d = Material constant.

$\Delta\varepsilon$ = Strain range, subscripts e, p, t and in represent elastic, plastic, total and inelastic strains, respectively.

T and C = Scaling factors in tension and compression, respectively.

a = Crack length correction under fatigue dominated failure.

m = Slope of plastic strain range versus cyclic life.

1/c = Cavitation correction factor under creep dominated failure.

G = Scaling factor under creep dominated failure.

C = Material constant.
σ_T = Tensile stress amplitude.
C_o, v_o, H and v = Material constants
ω = Total continuum damage
$\dot{\varepsilon}$ = Strain rate
0/0 = Continuously cycled R = -1 type of tests
t/0, 0/t, t/t and xt/yt = Time of hold in tension/compression.

INTRODUCTION

Creep-fatigue life prediction methods are very important, since they are used in the design and lifing of engineering components operating at high temperature. At least seven frameworks can be named within which a life prediction method may be developed:

1. Continuum damage mechanics
2. Phenomenological methods
3. Energy methods
4. Prediction of microscopic stress-strain
5. Fracture mechanics
6. Metallurgical and micro-mechanical modelling
7. Experience based empirical models.

The individual methods within the first six of the above frameworks use test parameters, stress-strain histories, strain rate or frequency and some form of damage such as 'crack' and its growth, in model formulation. Empirical methods use a model derived from the data or by experience. They can be extended to the life prediction of other materials. Hence, empirical methods do not have a scientific basis, but may be attractive as they do not require extensive specialized testing.

Requirements of creep-fatigue life prediction methods, their equations, the number of constants needed, together with the type of tests needed to apply them, have been reviewed in this paper. A new method has been developed with the ductility concepts and assessed with creep-fatigue data of five test materials.

LIFE PREDICTION METHODS

The prediction capability of a method depends on the percentage of the test data points (under different conditions) predicted within a band of ± x 2. The quality of the method increases with the number of points predicted within a factor of ± x 2. A logarithmic normal probability distribution of the ratio between the observed life and the predicted life of three austenitic stainless steels has been plotted by Wada *et al.* /1/ in Fig. 1, which shows that the design margin with a factor of 2 maintains the probability of non-failure above a 95% confidence level.

Life prediction methods have been extensively reviewed /2-10/, yet they have been sparingly assessed with various types of creep-fatigue data. Only two materials, 1Cr-Mo-V steel at 565°C /11/ and 2.25Cr-Mo steel at 600°C /12/, have been assessed with most popularly known methods of life prediction. Creep-fatigue data of no other alloy has been assessed with all these methods. Instead, the applicability of one or two methods has been assessed sparingly.

Phenomenological methods of life prediction are summarized below:

1) Damage Summation Approach (DSA) or Life Fraction Rule /13/.
2) Frequency Modified Approach or Separation Approach (FMA) /14/.
3) Strain Range Partitioning (SRP) Approach /15/.
   (a) Total Strain Version of (SRP) /16/.
   (b) Ductility Normalized SRP /17/.
4) Damage Rate Approach (DRA) /18/.
5) Hysteresis Energy Approach (HEA) /19/.
6) Damage Parameter Approach (DPA) /20/.
7) Modeling crack growth under creep fatigue /21,22/.

The problems one faces in using the above methods are the number of material constants and parameters which are usually unknown in the published literature. Hence, it is very important to address the requirements of the various life prediction methods.

METHODS AND THEIR REQUIREMENTS

Applying the phenomenological methods of life prediction to creep-fatigue data requires the following types of tests, where the constants are determined from the best fit equations.

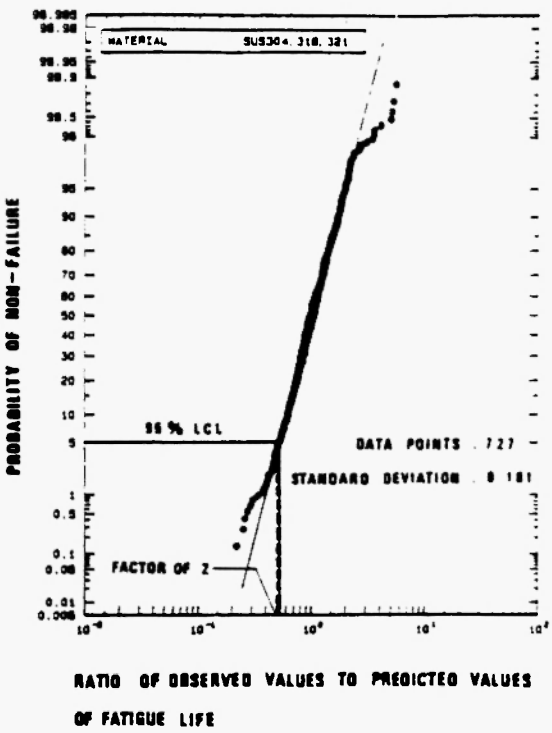

Fig. 1: Statistical confidence within a factor of ± x2 for creep-fatigue data on stainless steels 304, 316 and 321 /1/

1. Creep rupture properties at the same temperature relate stress-time (two constants in each linear behavior).
2. Stress relaxation with respect to hold time.
3. Total strain versus life data (four constants).
4. Elastic and plastic components versus life and respective constants (four in this case).
5. Stress range versus plastic strain. Slope (n) and the intercept (K) or fatigue strength constant, applicable above or below a plastic strain range.
6. Some of these tests with hold time sequences.
7. Apart from these, several constants that may be needed to apply a method, e.g., SRP needs eight such constants, inelastic strain components, versus life data.
8. Frequency versus life data.
9. Ductility under plasticity and creep.

Table 1 summarizes the individual methods, their equations, types of tests needed and number of constants of phenomenological methods of life prediction.

DUCTILITY – DEFINITION, MEASUREMENT AND MODELING

The American Society of Metals /24/ defines ductility as "the ability of a material to deform plastically before fracturing. Measured by elongation or reduction in area of a tensile test, by height of cupping in a cupping test or by radius or angle of bend in a bend test".

Measure of Ductility

"Currently ductility is considered a qualitative subjective property of a material" /25/. In general, measurements of ductility are of interest in three respects /25/:

1) To indicate the extent to which a metal can be deformed without fracture in metal working operations, for example, rolling and extrusion.
2) To indicate to the designer the ability of the metal to flow plastically before fracture. A high ductility indicates that the material is 'forgiving' and likely to deform locally without fracture should the designer err in stress calculations or the prediction of severe loads.
3) To serve as an indicator of changes in impurity level or processing conditions. Ductility measurements may be specified to assess material quality, even though no direct relationship exists between the ductility measurement and performance in service /25/.

Review of Modeling with Ductility

Manson /3,26/ used ductility in describing the low cycle fatigue properties of several materials. The universal slopes method /3/ used ductility to generate a point on the plastic line, whereas tensile strength and modulus were used to mark a point describing elastic behavior. The slopes of elastic and plastic lines were –0.12 and –0.6, respectively. Spreads in material response curves generated were in good agreement with above constants for a number of materials. Later Manson /27/ used the ductility term $(D)^{-0.15}$ to predict the strain hardening or softening behavior at the transition point by calculating the total strain and stress

Table 1
Requirements of phenomenological methods

Method of life prediction	Life prediction equation	No. of constants (n)	Details of the tests
Linear life fraction (13)	$1 = \sum N / Nf + \sum t / t_r$	- strain -life data (4) - creep-rupture (2 to 4)	0/0 tests (ε_t-Nf) creep rupture°C. stress relaxation
Frequency modified Approach (14)	$N_f = [F/\Delta\varepsilon_p]^{1/\beta'} [\nu_t/2]^{1-k}[\nu_c/\nu t]^{d}$	-strain-life data (4) - frequency vs. life (2) - stress-strain (2)	0/0 tests. some hold times frequency -life
Strain range partitioning (15).	$N_{ij}=A_{ij}\Delta\varepsilon_{ij}^{\theta jk}$ ij represent PP, PC, CP and CC loops.	four inelastic strain vs. life relations. (2x4)	Tests producing complex loops PP, PC, CP and CC.
Ductility Normalized SRP (17)		Plastic and creep ductility (2). and their exponents (2).	Tensile tests short time creep rupture tests.
Damage Rate Approach. (18). (no-creep damage)	$da/dN = a\,[T]\,[\varepsilon_p]^{m}\,[\dot{\varepsilon}_p]^{k}$ $da/dN = a[C]\,[\varepsilon_p]^{m}\,[\dot{\varepsilon}_p]^{k}$	scaling factors (2) strain -life (4) strain rate -life (2) assuming a crack size	0/0 tests. metallographic evidence. hold time tests.
with creep	$1/c\ da/dt = G\,[\varepsilon_p]^{m}\,[\dot{\varepsilon}_p]^{k'}$	scaling factor in creep cavity size (1) strain-life and rate (6)	metallographic evidence. creep data. test duration
Damage function method (19)	$C = \sigma_T \Delta\varepsilon_p N_f^{\beta} \nu^{\beta} (K-1)$	strain-life (4) frequency-life (2) stress-strain (2) shape correction factor	0/0 data. frequency data stress-life data hold time data.
Damage parameter approach (20)	$d\omega/dt = [\,Co\,\{\sigma/(1-\omega)\}^{V0}\,d\sigma/dt\ H(d\sigma) + C\{\sigma/(1-\omega)^{V}\}\ H(\sigma)$	material constants (3) fatigue -damage (2) creep-damage (2)	stress versus damage in creep and fatigue.

ranges. A neutral hardening stress range, corresponding to the transition strain range, was defined and an expression was used to predict hardening and softening, based on its being positive or negative /27/. Assessed with 30 materials, the prediction was in a reasonable agreement. Recently, Muralidharan and Manson /28/ simplified the method of universal slopes and extended it to lower strain levels by modeling with ductility.

Edmund and White /29/ assumed that failure occurred when the accumulated creep relaxation strains under cyclic-hold bend tests equalled the rupture ductility. This concept has been extended successfully in a modified form by Priest and Ellison /30/, Hales /31/ and Miller *et al.* /32/, applied to the creep-fatigue data of 1Cr-Mo-V and type 316 steel, to predict isothermal and thermo-mechanical fatigue lives. General expressions of creep and plasticity dominated failure were presented as follows:

$$N_c \Delta\varepsilon_{ct} = D_c \quad (1)$$

$$N_p \Delta\varepsilon_p = D_p \quad (2)$$

where subscripts p and c refer to fatigue and creep properties.

Halford *et al.* /17/ used ductility normalization with SRP and extended it to multiaxial creep-fatigue life prediction. Plastic and creep ductilities were determined for an environment from tension and short time creep-rupture tests, respectively. These were used in a set of damage normalized equations, which was the first order approximation of the four SRP inelastic life relations. Tensile ductility was used for the cycle types PP and PC, whereas creep ductility was used for CC and CP. Creep ductility is a function of exposure time and temperature which eventually decreases with longer time to rupture. A constant slope of −1.67 was kept for the ratio of inelastic strain range with ductility for cycle types PP and PC; however, inverse creep ductility was used for CC and CP. The transgranular and intergranular damage of a CP cycle was accounted for in the model in terms of a multiplier. Several parameters, such as environment and material parameters, were addressed adequately where a band in the predicted lives was observed from 2 to 4.

Viswanathan and Fardo /33/ reiterated that stress rupture ductility of many alloy systems at elevated temperatures varied with temperature and stress. Hence, short time tests cannot adequately predict the ductility of long-term stress-temperature conditions. They compiled a bank of rupture ductility data on Cr-Mo steels and obtained statistically viable best fit equations. One was an empirical quadratic model in stress and temperature, which predicted % RA at rupture. In the second model, percent RA varied linearly with stress such that the slope was independent of temperature, but the intercept varied exponentially with (1/T) and was successful in describing the data over a limited range of RA.

Tipler and Hopkins /34/ studied the cavitation and rupture ductility of Cr-Mo-V steels. They observed that lower elongation is associated with higher density of cavities per unit strain. A large scatter in the data was also reported.

Roan and Seth /35/ investigated the residual impurity effects on grain boundary cavitation, fracture behavior and associated rupture life and ductility of Cr-Mo-V steel. They observed that different impurities affect rupture ductility to different extents. Individual elements and their contribution to rupture ductility, cavitation and fracture mode were accounted for by 'total effective impurity content'. The % RA decreased linearly as the total effective impurity contents (%) increased. The % RA also decreased linearly with cavities per grain. By combining these two results they showed that lowering the impurity content lowered the number of cavities per grain and in turn improved ductility. However, there are conflicting opinions /36,37/ that, by refining the grain size, cavities per grain may be reduced effectively, which is unlikely /35/, since increasing the number of grains at the same impurity content may increase the cavity density and leave rupture ductility unaffected.

Rhines and Wray /38/ noticed that, under proper conditions of test temperature and strain rate, a dip in ductility in an intermediate temperature range occurs. This was due mainly to a rapid drop off in total elongation just above the recovery temperature. They postulated that when the ductility is high at low temperatures, fracture occurs by transgranular crack propagation with extensive deformation. At intermediate temperatures, deformation occurs by grain boundary shear, and intergranular voids form at triple points and grow unhindered to produce intergranular

failure. This causes a minimum in ductility. At higher temperatures recrystallization occurs simultaneously with intergranular void formation that continuously breaks up the path of intergranular cracking. This results in a gain in ductility. Later some of these findings were verified by several other workers /39-41/.

Hammond /41/ related tensile properties, such as yield and tensile strength and % elongation, with toughness, which in turn is a product of strength and ductility. He investigated the effect of prolonged aging on the inversion of total elongation and diminishing ductility behavior of the superalloy Haynes alloy no. 25. He also found ductility minima and their reversals pronounced at approximately one-half the absolute melting temperature. Sikka /42/ determined that certain combinations of strain rate and test temperature can result in a significant loss in elevated temperature ductility of the stainless steel types 304 and 316, respectively. The strain rate below which ductility drop was initiated decreased with decreasing temperature. Besides strain rate and test temperature, ductility also increased with nitrogen content and thermal aging.

DEVELOPMENT OF DUCTILITY MODEL

Several parameters affect the material ductility, for example,

1) strain rate
2) strain range
3) temperature
4) material heat and conditions
5) impurity content
6) cavities per grain
7) grain size
8) tensile and compressive stress ranges
9) relaxed stresses
10) phenomena such as work hardening, recovery, recrystallization, coarsening, formation of grain boundary precipitations, dislocation density and their mobility for cell formation.

Incorporation of the above parameters will not lead any model towards generalization, since each material has a different composition and metallurgy. Several assumptions have been made in developing the ductility model. These are discussed below:

1) Stress in tension and compression has been separated and has been plotted with respect to strain range to rate ratio, which is 'cycle time' shown in Fig. 2.
2) Cycle types, such as trapezoidal, triangular, square and sinusoidal waveforms, have been treated as rectangles with simplification of the waveform as shown in Fig. 3.
3) The product of stress range and strain range-to-rate ratio or cycle time (dynamic viscosity) in tension and compression has been determined with the lowest strain rate in either direction. Lower strain rate also means longer cycle time and more energy accumulated.
4) Only one part of the cycle (tension/compression) was assumed to contribute to the accumulation of damage.
5) The dynamic viscosity was integrated for the cycles to failure. This was achieved from the expression of stress-strain, in terms of the Basquin equation, that has an intercept K (fatigue strength coefficient) which is the stress range at 1 inelastic strain range and the strain hardening exponent (n).
6) The fatigue strength constant (K) was assumed in the literature as $3.5\sigma_u$; through empirical adjustments, 3.5 was replaced with (log $A+D_t$), adding the logarithmic intercept of continuous fatigue (0/0) behavior with tensile ductility at the creep-fatigue test temperature.
7) Subsequent terms are strain-based, using total strain and strain rate (1/sec) in absolute scale integrated for cycles to failure.
8) A work hardening correction factor (H) was introduced to account for the fatigue process, which in turn depends on hardening, softening and phenomena like recovery and recrystallization, in terms of yield to tensile strength ratio and hold time.
9) With strength ratio improvement or otherwise, the rate of work hardening is influenced. Hold containing cycles affect the work hardening response which is inhibited by softening processes

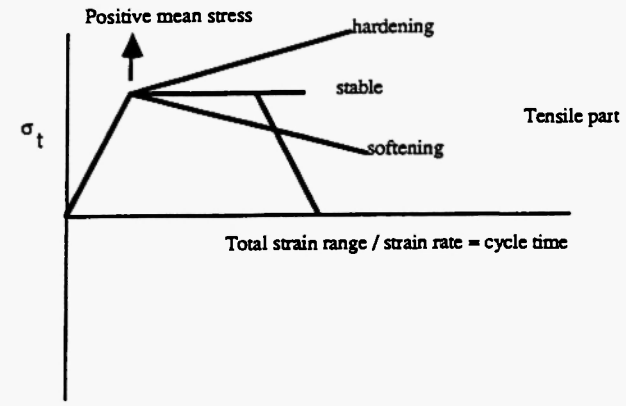

(a) Possible trends in the stresses in tension direction.

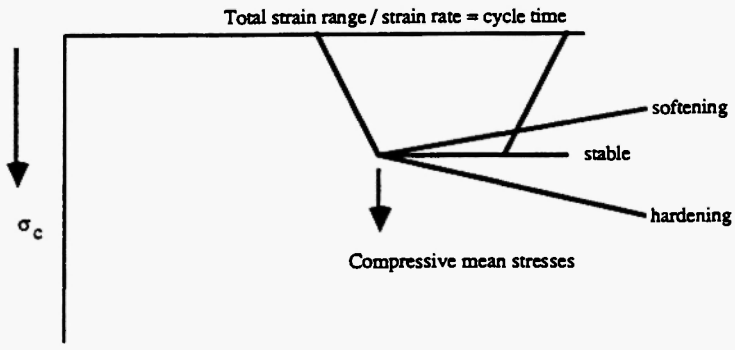

(b) Possible trends in compression direction.

Fig. 2: Schematic representation of stresses in two directions.

and is accounted for in the expression for H. This parameter was determined empirically.

10) The dynamic viscosity has been equated with material toughness, which is a product of tensile strength and ductility.
11) Ductility was assumed in terms of the product of plastic strain range and cyclic life, given in equations (1) and (2).

Following these assumptions, the ductility model was developed as follows:

For Variable Strain Rate:

On many occasions, in the case of unbalanced cycles, tensile and compressive strain rates were different, and so were the hold times in either direction. The lowest strain rate reflects greater energy

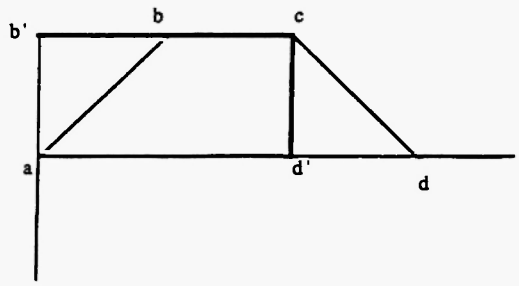

(a) Approximations in area calculations of a trapezoidal cycle

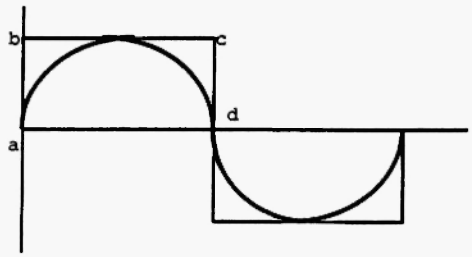

(b) For a sine waveform the rectangular area calculation.

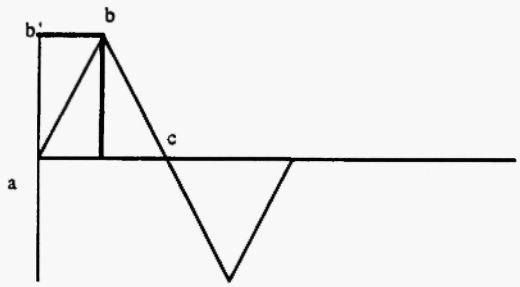

(c) Approximation in area calculations for a tringular cycle

Fig. 3: Approximations in area calculations for different waveforms.

accumulation, and accounts for the longer cycle time in the direction of the hold.

$$\text{Dynamic viscosity} = \Delta\sigma\Delta\varepsilon(\dot{\varepsilon})^{-1} \quad (3)$$

Waveforms were simplified in terms of conventional rectangles. Such an area under the tensile part of a trapezoidal cycle (abcd) was assumed a rectangle (ab'cd'), as shown in Fig. 2(a), and was integrated for cycles to failure.

$$= \int \Delta\sigma\Delta\varepsilon(\dot{\varepsilon})^{-1}$$
$$= K(\Delta\varepsilon_{in})^{n}.(\Delta\varepsilon_{t})^{m}.(\dot{\varepsilon})^{-m} \quad (4)$$

where m is the slope of total strain versus life under 0/0

Table 2
Requirements of proposed ductility model

Method of life prediction	Life prediction equation	No. of constants (n)	Details of the tests
Ductility model	$N_f = (A+D_t)\,(\Delta\varepsilon_{in})^{n-1}$ $.(\Delta\varepsilon_t)^{m}\,(\dot{\varepsilon})^{-m}.H$	Total strain Vs. Life (2) Stress Vs. strain (2) Mechanical properties	Total strain 0/0 Tensile tests.

conditions. The fatigue strength coefficient was empirically adjusted as follows:

$$K = 3.5\,\sigma_u$$
$$K = (\log A + D_t)\sigma_u \qquad (5)$$

where logA is the intercept of total strain versus cyclic life for continuous fatigue, D is the tensile ductility at test temperature and n is the cyclic hardening exponent.

$$\text{Material Toughness} = \text{Ductility x Tensile Strength} = \Delta\varepsilon_p \,.\, N_f \,.\, \sigma_u \qquad (6)$$

Combining equations (5) and (6),

$$N_f = (A+D_t)\sigma_u(\Delta\varepsilon_{in})^n(\Delta\varepsilon_t)^m\,(\dot{\varepsilon})^{-m})\,H/\Delta\varepsilon_{in}\sigma_u \qquad (7)$$

Simplifying equation (7) results in

$$N_f = (A+D_t)(\Delta\varepsilon_m)^{n-1}.(\Delta\varepsilon_t)^m\,(\dot{\varepsilon})^{-m}.H \qquad (8)$$

The work hardening correction factor (H) included in equations (7) and (8) accounts for the hold times (t_h) expressed in the following empirical form:

$$H = \sqrt{[1+(\mathrm{Log}(1+(\sigma_y/\sigma_u)+t_h)^m]} \qquad (9)$$

where hold time is in sec., and the other parameters have their usual meanings.

There is a lack of understanding of 'work hardening', its measurement and its effects on the fatigue resistance of materials. Phenomena such as work hardening inhibitor or softening by recovery are also not known quantitatively. Hence, empirical adjustments were made. Fewer data points are required to determine the slope of total strain (between 2% to 0.6%) versus cyclic life. Using these details from continuous fatigue behavior in the model, life of hold containing cycles can be predicted.

DISCUSSION ON THE APPLICABILITY OF THE PROPOSED METHOD

Creep-fatigue data have been collected /43/ to assess the applicability of a new method developed in this paper. These are summarized in Table 3.

Total strain versus life relations of the above materials are determined under continuous fatigue conditions, having the following form:

$$\Delta\varepsilon_t = A(N_f)^m \qquad (10)$$

The intercept (A) and slope (m) are tabulated in Table 4.

A small program was written in Excel to calculate the life of pure fatigue and complex combinations of hold time cycles. The prediction capability of the method is as follows:

AMZIRC: Life prediction of creep-fatigue data of AMZIRC is shown in Fig. 4. At least 66% of the test data points were predicted within a factor of ± x2, 30% in a band of 3 and only one data point which constitutes 3% of the data was within a factor of 7, in a compressive dwell sequence of 300 sec., applied at 4.6% total strain range.

The prediction capability of the proposed method with the cycles containing hold in tension or compression time is quite good, 70% of the test data points belonging to a factor of ± x2, 23% within a

Table 3
Summary of the materials assessed and their properties

Materials	Test Temperature °C	Yield strength MPa	Tensile strength MPa	Ductility at test temperature %
AMZIRC	538	212.5	216.5	1.83
IN 100	650	1034	1200	0.22
Waspaloy	750	828	1091	0.38
Ti-6Al-4V	450	637	729	0.67
1Cr-Mo-V	565	400	500	1.6

Table 4
Continuous fatigue (total strain versus life)
behavior of the materials

Materials	m	log A
AMZIRC	-0.58	2.2
IN 100	-0.23	0.82
Waspaloy	-0.4	0.99
Ti-6Al-4V	-0.256	0.96
1Cr-Mo-V	-0.57	1.78

factor of 3 and the remaining 7% within a factor of 7. The standard error, together with the equivalent factor on life, have been tabulated in Table 5.

IN 100: Creep-fatigue data of powdered (PM) IN 100 were assessed with the proposed method in Fig. 5. 70% of the test data points are predicted within a factor of ± x2. Figure 5 also contains the details of the points that do not fall within a factor of ± x2. Longer tensile dwell cycles with 3600 to 7200 seconds have been over-predicted within a factor of 3. The remaining 30% of the test data points are predicted within a factor of 3, summarized in Table 5.

Waspaloy: The life prediction is shown in Fig. 6. A life range of ± x2 to 30 is observed. Only 44% of test data points are predicted within a band of ± x2. The rest of the breakup is as follows: 24% within a factor of 3, 6% within a factor of 5 and 3% within a factor of 7, 12 and 30, respectively. Only unbalanced dwell sequences with 100 seconds in tension and 10 seconds in compression were predicted within a factor of ± x2. Only one condition of compressive hold cycle from a group of six was within a factor of ± x2. Two conditions of tensile dwell sequences from a batch of five were within a factor of ± x2 and only one balanced dwell data point, which represents 20% of the data, was within a factor of ± x2.

Ti-6Al-4V: A complex combination of hold times in the tension and compression directions has been assessed in Fig. 7. 76% of the test data points were predicted within a factor of ± x2 and the remaining 24% within a factor from ± x2 to 3. The lowest strain rate of either tension or compression direction in the model effectively predicts the life of either tensile, compressive, balanced or unbalanced cycles. Prediction capabilities have been tabulated in Table 5.

1Cr-Mo-V Steel: Not all the parameters were

Table 5
Statistical distribution in the life prediction by proposed method

	Proposed method		Life extrapolation Eq. (10)	
Materials	Standard error	Equivalent factor on life	Standard error	Equivalent factor on life
AMZIRC	0.01149	1.026	0.012	1.027
IN 100	0.0064	1.014	0.031	1.073
Waspaloy	0.134	1.362	0.029	1.198
Ti6Al4V	0.051	1.125	0.009	1.021
1Cr-Mo-V	0.099	1.258	0.129	1.345

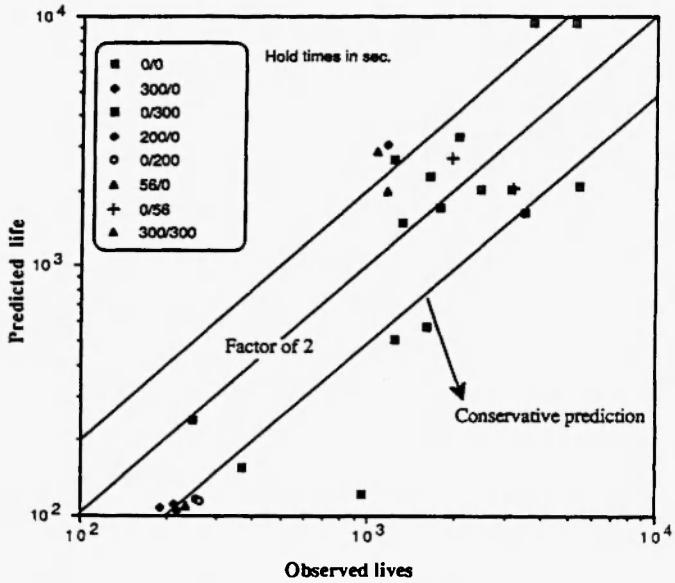

Fig. 4: Life prediction of AMZIRC by proposed method.

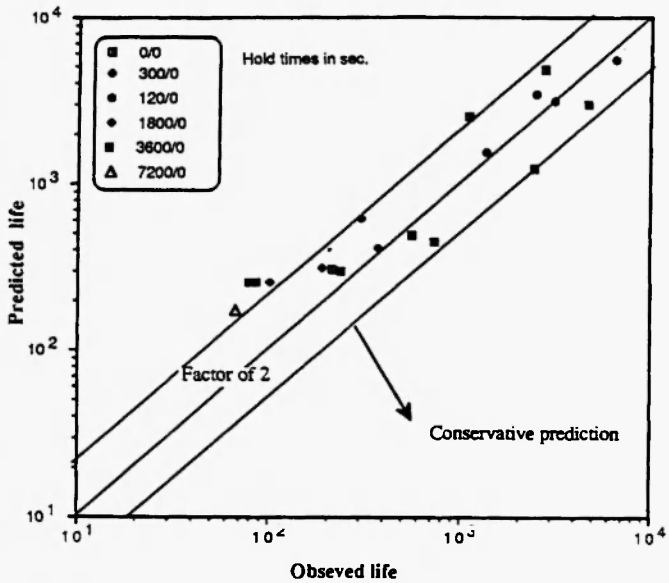

Fig. 5: Life prediction of IN 100 by proposed method.

known for this particular set of data, where very long hold times were applied in either direction with or without hold in the opposite direction. Constant strain rate conditions apply to this material. Life prediction is shown in Fig. 8. The standard error calculated with an equivalent factor on life is tabulated in Table 5.

The five test materials chosen represent a wide range of material properties. For example, AMZIRC has a very high yield-to-tensile strength ratio, close to one, and the plastic strain component is much higher than the elastic one as opposed to that of IN 100 (powder compact), where both the total strain and elastic strain components are nearly the same. There is also an intermediate band of strain levels where elastic and inelastic strain components vary with respect to the total strain level of Waspaloy, Ti-6Al-4V and 1Cr-Mo-V. Below 0.4% total strain level, the elastic strain component is much higher than the plastic component for these materials.

The discrepancies in the predicted life of hold containing cycles cannot be explained for AMZIRC, since over-predicted cycles have similar strain rates. The plastic strain component is very near the total strain component, and the role of relaxed stresses, which account for 50% of the half life tensile or compressive stresses, needs to be accounted for. A high yield-to-

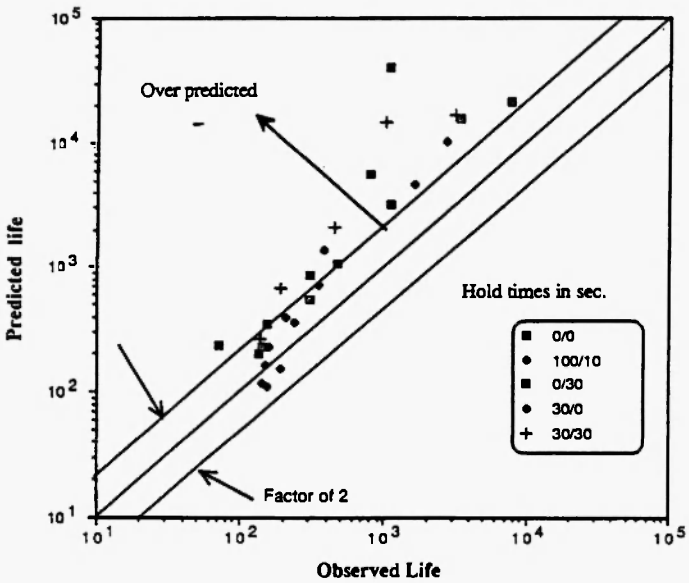

Fig. 6: Life prediction of Waspaloy by proposed methods.

time of hold, it usually exceeds unity. There is no direct incorporation of the relaxed stresses and inelastic strain build-up in the model to account for the hold times. However, this contributing factor for the life reduction has been accounted for in terms of H.

The predicted life in the case of IN 100 with hold times of 3600 seconds or more was overpredicted within a factor of 3. Though those cycles also have strain rates similar to those of other cycles, within a total strain range from 0.85% to 1.5% and inelastic strain ranges from 0.012% to 0.342%, it was observed that, as the inelastic strain levels increased from 0.25%, the cyclic lives were over-predicted within a factor of 3.

Within a range of yield-to-tensile strength ratio of 0.85 - 0.87, prediction by this method has been found quite good for two materials, namely, IN 100 and Ti-6Al-4V. In the case of Ti-6Al-4V, only tensile dwell cycles were under-predicted within a factor of 3 and

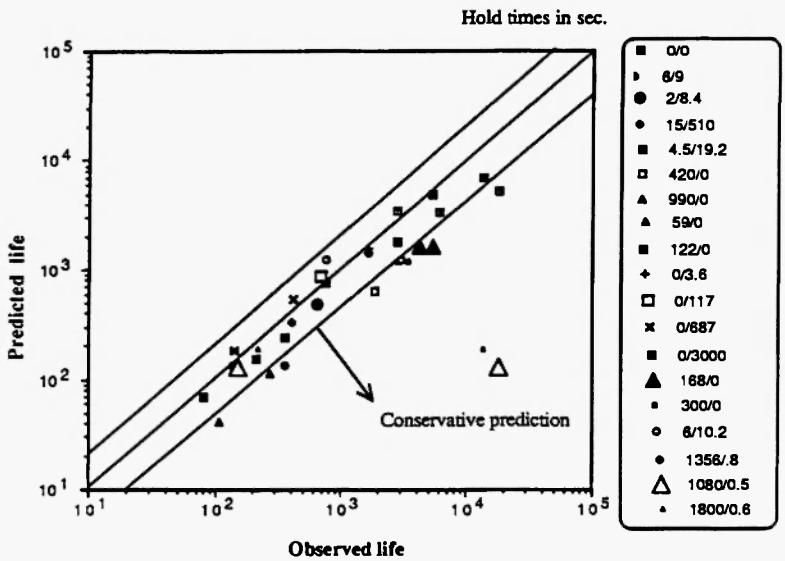

Fig. 7: Life prediction of Ti-6Al-4V by proposed method.

tensile strength ratio is a direct measure of work hardening, which allows stable plastic deformation. With such high work hardening ratios, a simultaneous softening process, such as recovery or recrystallization, often operates since work hardening is inhibited resulting in an ultimate tensile strength close to yield. A contribution to ductility in such cases arises from the plastic instability region. Though the factor 'H', which accounts for the hold times, decreases with increasing unbalanced cycles with compressive hold times more than the tensile part were under-predicted within a factor of 3. In this range of strength ratios, the phenomenon such as work hardening is favorable; however, this may be inhibited by the aluminium content in the solid solution as it decreases the tendency for dislocation tangle and cell formation /44/. The degree of work hardening/softening for the above materials is unknown and a quantification to ductility

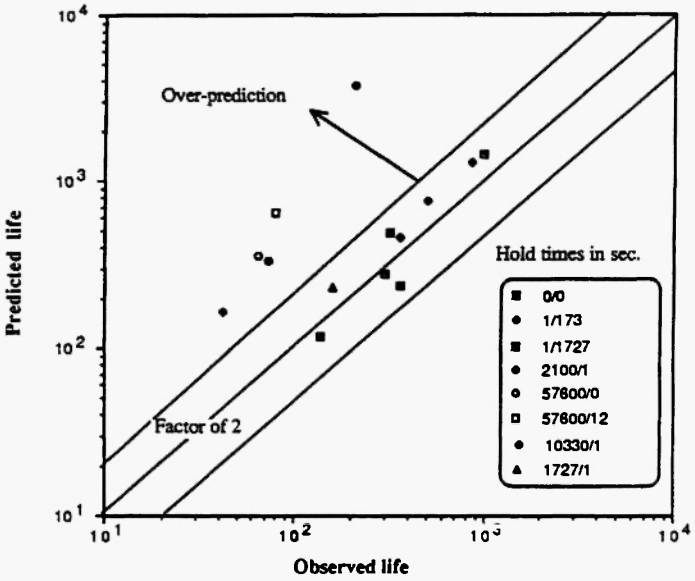

Fig. 8: Life prediction of 1Cr-Mo-V by proposed method.

enhancement or otherwise is unknown.

Two materials, 1Cr-Mo-V and Waspaloy, have strength ratios in the range of 0.8 to 0.75, respectively, and the predicted life has been over-predicted for both materials. The work hardening behavior and its inhibitor mechanisms which either increase or decrease the life are not known. The ductility, which is derived from work hardening factor H, over-estimates the material fatigue ductility and resulting properties and hence the proposed method does not account for the lower strength ratios below 0.8 and for cases with complexities in part of the test parameters. Since this method needs a few tests under total strain control, the factor n will also be determined from the same tests.

CONCLUSIONS

1) The proposed model predicts the creep-fatigue lives within a reasonable acceptable band of ± x2. However, prediction by this method is not very encouraging for materials with an intermediate range of strength ratios.
2) An account of variable strain rate has been made in the model which accounts for the hold times. Using the variable strain rate considerations, life is over-predicted for materials within a range of strength ratios.
3) The work hardening correction factor term that has been incorporated in the model remains constant for the continuous fatigue cycles; however, for hold time cycles it decreases.
4) Further work is needed to account for the ductility and its measurement under high temperature fatigue. The effect of work hardening on life improvement or otherwise with mechanisms such as softening by recovery or recrystallization within a range of strength ratios calls for further investigations.

ACKNOWLEDGEMENT

Discussions with Dr. Gary R. Halford of NASA Lewis Research Center are gratefully acknowledged.

REFERENCES

1. Y. Wada, Y. Kawakami and K. Aoto, "A statistical approach to fatigue life prediction for SS 304, 316 and 321 Austenitic stainless steels", in: *Material Deformation and Thermo-Mechanical Fatigue,* H. Sehitoglo and S.Y. Zamrik (eds.), ASME, 1987; pp. 37.
2. S.S. Manson, "A critical review of predictive methods for treatment of time dependent metal fatigue at high temperature", in: *Pressure Vessel and Piping Design Technology – A Decade of Progress,* S.Y. Zamrik and C. Dietrich (eds.), ASME, 1982; pp. 203.
3. S.S. Manson, *Exp. Mech.*, 5, 1933-226 (1965).
4. E.G. Ellison, *J. Mech. Eng. Society,* 11 (3), 318 (1969).
5. C.R. Brinkman, *Int. Metals Review,* 30 (5), 235 (1985).
6. T. Bui-Quoc and A. Biron, *J. Nucl. Engng. and Design,* 71, 135 (1982).
7. G.R. Halford, T.G. Meyer, R.S. Nelson, D.M. Nissley and G.A. Swanson, *ASME Trans. J. Engng. Gas Turbine & Power,* 111, 279 (1989).

8. J.L. Chaboche and C. Levaillant, *Nucl. Engng. Design*, **83**, 279 (1984).
9. T. Goswami, "Review of High Temperature Low Cycle Fatigue Life Prediction of Low Alloy Steels", Report submitted to the Electricity Commission of New South Wales, Sydney, Australia, 1990.
10. D.A. Miller, R.H. Priest and E.G. Ellison, *High Temper. Mater. & Processes*, 6 (3-4), 155 (1984).
11. E.G. Ellison and A.J.F. Paterson, *Proc. Institution of Mechanical Engineers*, **190**, 321 (1976).
12. T. Inoue, T. Igari, M. Okazaki and K. Tokimasa, *Nucl. Engng. Design*, **114**, 311 (1989).
13. American Society of Mechanical Engineers, "Code Case N-47 ASME Boiler and Pressure Vessel Code", 1974.
14. L.F. Coffin, *Proc. Institution of Mech. Engineers*, London, 9, 74; 1974; pp. 188.
15. S.S. Manson, G.R. Halford and M.H. Hischberg, "Creep-fatigue analysis by strain range partitioning", *Symposium on Design for Elevated Temperature Environment*, ASME, 1971; pp. 12. (also as NASA TMX 67838).
16. S.S. Manson and R. Zab, "Treatment of low strain and long hold times in high temperature material fatigue by strain range partitioning technique", ORNL /sub/3988, Case Reserve Western University, Ohio, 1977.
17. G.R. Halford, J.F. Saltsman and M.H. Hirschberg, "Ductility normalized strain range partitioning life relations for creep-fatigue life predictions", NASA TM 37377, 1977.
18. S. Majumdar and P.S. Maiya, "A unified and mechanistic approach to creep-fatigue damage", ANL report, 76 / 58, 1976.
19. W.J. Ostergren, *J. Testing and Evaluation*, 4, 327 (1976).
20. N. Chrzanowski, *Int. J. Mech. Science*, 18, 69 (1976).
21. S.D. Antolovitch, S. Liu and R. Baur, *Met. Trans.*, 12A, 473 (1981).
22. Y. Oshida and H.W. Liu, in: *Low Cycle Fatigue – Direction for the Future*, ASTM STP 942, 1989; pp. 1199.
23. T. Goswami, Papers I through III, *High Temperature Materials and Processes*, **14** (1), 1, 21, 35 (1995).
24. G.E. Dieter, "Mechanical Behavior of Materials Under Tension", American Society for Metals, Metals Handbook, 8, Mechanical Testing, 1985.
25. G.E. Dieter, "Introduction to ductility" in *Ductility*, ASM, 1968.
26. S.S. Manson and G.R. Halford, *Israel J. Tech.*, **21**, 29 (1983).
27. S.S. Manson, *Int. J. Fracture Mech.*, 2, 327, (1966).
28. U. Muralidharan, *J. Testing and Evaluation*, **16** (2), 146 (1988).
29. H.G. Edmund and D.J. White, *J. Mech. Eng. Sci.*, **8** (3), 310 (1966).
30. R.H. Priest and E.G. Ellison, *Mat. Sci. & Eng.*, **49**, 7 (1981).
31. R. Hales, *Fat. Energ. Mater. Struct.*, **6**, 121 (1983), also as CEGB Report No. TPRD/ B/ 0038/N82 (1982).
32. D.A. Miller, C.D. Hamm and J.L. Philips, *Mat. Sci. & Eng.*, **53**, 233 (1982).
33. R. Viswanathan and R.D. Fardo, "Parametric techniques for extrapolating rupture ductility", *Ductility and Toughness Considerations in Elevated Temperature Service*, Winter Annual Meeting of the ASME, G.V. Smith (ed.) (1978).
34. H.R. Tipler and B.E. Hopkins, *Metal Science*, 47 (1976).
35. D.F. Roan and B.B. Seth, "A metallographic and fractograpahic study of the creep cavitation behavior of 1Cr-1Mo-0.25V rotor steels with controlled residual impurities", *Ductility and Toughness Considerations in Elevated Temperature Service*, Winter Annual Meeting of the ASME, G.V. Smith (ed.), 1978.
36. P.G. Stone and J.D. Murray, "Metallurgical aspects of ferritic bolt steels", in: *High Temperature Properties of Steels*, Publication 97, Iron & Steel Institute, London, 1967; pp. 483.
37. J. Glen and J.D. Murray, "Metallurgical aspects of creep in carbon and low alloy steels, Special Report *Symposium on Steels for Reactor Pressure Circuits*, Iron & Steel Institute, London, 1961; pp. 40.

38. F.N. Rhines and P.J. Wray, *Trans. Amer. Soc. for Metals*, **54**, 117 (1961).
39. E. Shapiro and G.E. Dieter, *Metallurgical Trans.*, **1** (6), 1711 (1970).
40. M.A. Arkoosh and N.F. Fiore, *Metallurgical Trans.*, **3** (9), 2235 (1972).
41. J.P. Hammond, "Ductility minimum and its reversal with prolonged aging in cobalt and nickel base superalloys", *Ductility and Toughness Considerations in Elevated Temperature Service*, Winter Annual Meeting of the ASME, G.V. Smith (ed.), 1978; p. 63.
42. V.K. Sikka, "Elevated temperature ductility of types 304 and 316 stainless steel", *Ductility and Toughness Considerations in Elevated Temperature Service*, Winter Annual Meeting of the ASME, G.V. Smith (ed.), 1978; pp. 129.
43. AGARD CP 243, "Characterization of High Temperature Low Cycle Fatigue by Strain Range Partitioning Technique", 1978.
44. N.S. Stoloff, "Fracture of iron base solid solution alloys", in: *Proc. Conference on the Physical Basis of Yield and Fracture*, Oxford, 1966. Institute of Physics and Physical Society, London, 1968; pp. 68.